An Experimentally Based Characterization of Solar Cell Structure Defects by Means of Noise and Optical Activities Analysis

Robert Macku [1,a], Jiri Sicner [1,b] and Dinara Sultanovna Dallaeva [1,c]

[1] Brno University of Technology, Faculty of Electrical
Engineering and Communication, Department of Physics
Technicka 8, 616 00 Brno, CZECH REPUBLIC

[a] macku@feec.vutbr.cz, [b] xsicne02@stud.feec.vutbr.cz, [c] xdalla02@stud.feec.vutbr.cz

Keywords: Solar cell; light emission; breakdown; fracture; silicon; noise; diagnostics.

Abstract. This paper will be discussed the issue of non-destructive testing of silicon solar cells structure. The fabricated devices generally exhibit lots of different imperfections that limit the ability to apply new composite materials and technological approaches. We demonstrate high sensitive electrical noise measurement philosophy with strictly non-destructive character in order to identify defects physical nature. Main parameters in the view are excess leakage current and electric noise, live-time and reliability reduction and finally decreasing of conversion efficiency. Here will be presented relations between the specimen transport characteristic and electric noise generated in consequence of the local electric breakdowns in the affected regions. In addition, we are able to show that fracture-based defects are attended by the low intensity light emission especially in visible and deep infrared wavelength range. Nevertheless, optical activity physical nature is in a question. For this reason we will present also measurement of optical spectra radiation and optical intensity vs. voltage bias and temperature to introduce different defect phenomena interpretation.

Introduction

The photovoltaic electricity for the terrestrial application as a green energy sources was introduced in 1970s. Very early turned out that the low-scale production process used before for space program are strongly inconvenient. At the time also arisen new problems associated with the cost of production, radiation spectrum modification by absorption in the atmosphere, conversion efficiency as a function of the radiation intensity and choice of suitable materials. In recent years, we observe a rise in the production of solar modules about (30 ÷ 40) % per year and the cost reduction between (5 ÷ 7) %, [1], [2]. Despite to the level of effort on innovations of manufacturing processes there is huge discrepancy between the laboratory and industry based solar cells. The main problems are related to the efficiency and defects reducing the life-time and reliability. This is compounded by the lack of a comprehensive scientific base for an interpretation of specific defects in the structure due partly to large scale manufacturing process and new materials. This lack of systematic science base has been the biggest hindrance to the progress in the photovoltaic and innovations have been often empirical. Several authors such as Koktavy, [3], and Chynoweth, [4], provides interesting systematic research on low dimension semiconductor barrier-like devices. Nevertheless, application of related approaches and conclusions to solar cells is still in question. On the other hand, Breitenstein, [5], and Skarvada, [6], published treatise on solar cells mechanical-based structure defects and/or cracks. They have used extended microscopy methods and lock-in thermography to detect mesoscopic and microscopic defect region. Note that their research is based mostly on optical inspection of the surface apparent defects. Our approach is based mainly on the application of excess noise signal measurement and finding of correlations with transport and optical characteristics to provide

physical interpretation. We managed to identify several diagnostically interesting defects in the solar cell structure. The first of them are particularly dangerous in terms of the sample degradation or destruction. The flowing current is very high as well as power dissipation and there is threat of the structure melting. Negative temperature dependence of the breakdown voltage indicates carriers tunneling of thermal instabilities, [7]. Observed noise in the frequency domain shows 1/*f* fluctuation in the low frequency region. We have also measured that other defects are strongly dependent on the electric field. We discovered that when a high electric field is applied to a pn junction containing some technological imperfections, local breakdowns arises in micro-sized regions, which in turn can lead to the deterioration in quality or destruction of the pn junction. It is therefore advisable to use methods which can indicate the presence of these regions in the pn junction and suggest the quality assessment and quantitative description of tested solar cells possible.

Experimental Details

Electrical noise and transport characteristics measurement. The nature of the observed noise depends on the voltage (current) bias applied to solar cells. This can be attributed to variations in the electric stress and origin of breakdowns. Thanks to this fact, our study is strictly divided into reverse and forward bias conditions. With regard to the paper scope here will be studied only reverse-biased specimens.

The solar cell bias voltage is provided by a high-precision laboratory power supply. Its output voltage must be filtered because of the presence of additive noise types. The filter cut-off frequency is approx. 1 Hz. The specimen under investigation is placed in a dark environment; it is electrically shielded and it is kept at a constant temperature (16.6 ± 0.2) °C to avoid self-heating. A pick-up resistor R_L to measure the specimen current fluctuations, is connected in series with the specimen (R_L = 5.36 Ω). The simplified circuit diagram is depicted in Fig. 1. The noise voltage is amplified by means of low-noise amplifiers (PA31 – gain 20 dB, cut-off frequency 10 MHz; EG&G 5113 – gain 30 dB, cut-off frequency 1 MHz) and measured by means of a selective nano-voltmeter (Signal Recovery Model 7310) or alternatively by FFT dynamic spectral analyzer Agilent 35670A. For very sensitive measurement is used also a Signal Recovery ultralow noise preamplifier 5184. From the procedure viewpoint, the approach remains the same in both cases. The nature of noise will be appraised on the basis of the measurements of the double-sided noise power spectral density (PSD).

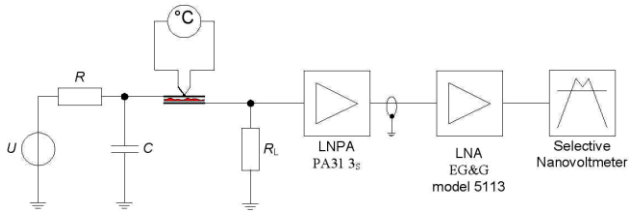

Fig.1. Simplified circuit diagram of experimental arrangement for noise measurement. Here *U* is the bias voltage supply, LNPA is the low-noise pre-amplifier, LNA is the low-noise amplifier.

Transport characteristics are measured by means of the National instruments PXI module 4130. Formally, it is single measurement unit including voltage (current) source and voltmeter (alternatively ammeter). Specific future of this device is operation in all four quadrants and it provides the voltage offset compensation for the low voltage measurement. An external lead-acid battery as a primary power source is used especially for the low noise measurement. The output noise voltage at 25 Hz is only 45 μV/Hz (DC voltage 1 V) and 58 μV/Hz if 10 V is selected.

Optical properties measurement. The radiation generated from reverse-biased pn junction defects is used to study local properties (far field detection). It proves to be useful to measure surface radiation and to make light spots localization also to measure the radiation intensity versus voltage plot, its correlation with other, mainly noise characteristics and the radiation spectrum. To this aim a scientific CCD camera G2-3200 with a 3.2 MPx resolution was used for measuring of the radiation from a pn junction solar cell surface. It uses a silicon chip cooled by dual system of Peltier's modules with the operation temperature down to -50 °C. The Dark current of an optical sensor and a single pixel is 0.8 e/s (it holds for T = 0 °C). The dynamic range of the elementary pixels with a usable range up to 16 bits is very good. A camera lens with focal ratio 1.2 and working aperture 41.7 mm is used with the camera. It is possible to measure in the useful range of wavelengths of 300 nm – 1100 nm. Since the producer defines the spectral characteristics of the particular CCD chip, photometry measurements can be performed as in our case. The CCD Camera together with the solar cell sample is in the optically shielded chamber (see Fig. 2). The sample temperature is kept constant during the measurement by the PID temperature regulator integrated in the Keithley source meter. The sample bias is realized by the constant voltage source controlled via IEEE 488.2 bus.

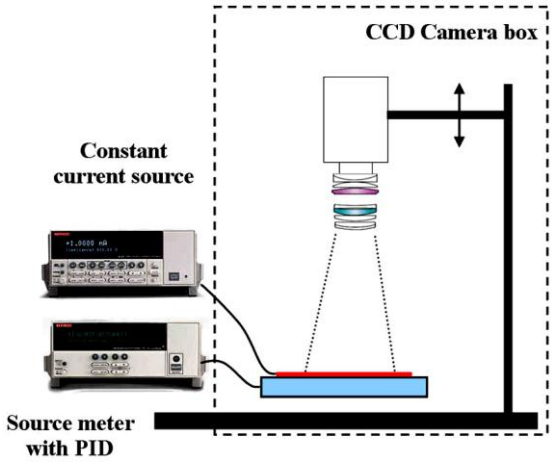

Fig.2. Experimental set-up for optical activities registration.

Related experimental apparatus is based on the infrared camera Micro-Epsilon TIM 160. The spectral range (7.5 ÷ 13) μm provides information about defects thermal radiation according to the Planck's Law. It uses the same temperature stabilization and the bias source as an astrological CCD camera set-up. The infrared camera allows real-time thermography view with the 120 Hz frame rate and a thermal sensitivity about of 0.08 K. By this way it is possible to study a defect time development and pre-breakdown phenomena.

Results and discussion

Study of defect thermal properties. The first results presented here will be connected with local defect spots localized outside the edges regions. Solar cells specimens are prepared with a view of edges leakage effects suppression. This phenomena indirectly gives arise of photon activity as a result of a surface recombination and conductive channel thermal radiation. This behaviour is diagnostically difficult to use because we are unable to distinguish surface and bulk current components. Figure 3 depicts the thermal radiation of the solar cell sample M5 which includes only one defect spot close to the edge. Note that defect thermal nature must be specifically discussed. Generally, bolometric based infrared cameras are not selective to collect only deep infrared radiation and spurious direct recombination mechanisms may induce a wandering thermal picture. By means

of an infrared filters (optical bandwidth 100 nm) has been studied spectral distribution of a radiation and the thermal radiation was confirmed.

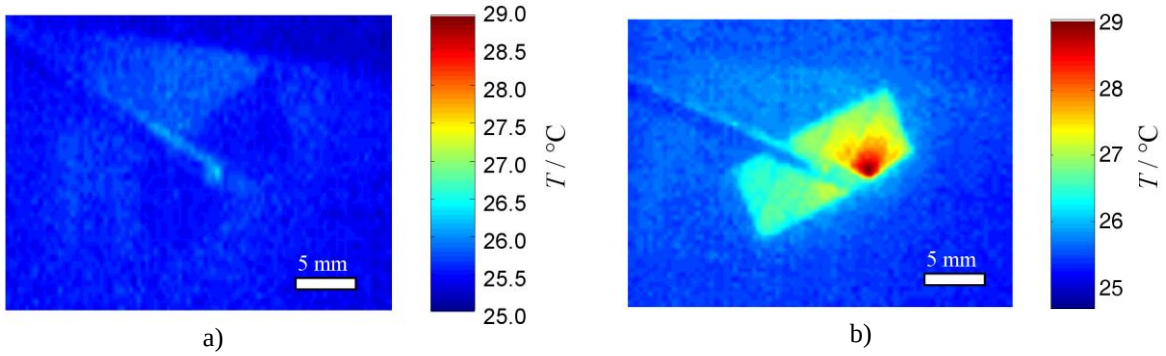

a) b)

Fig.3. Thermal activity of solar cell sample M5; a) bias voltage U_R = 1 V; b) U_R = 16 V. Sample holder was kept at constant temperature T = 25.0 °C. Solar cell emissivity ε = 0,91.

The thermal radiation of whole sample increases along with an excess reverse current I_R and the defect spot is allowed to be activated by the local current density and the local overheating. The local conductive channel concentrates current from neighbourhood and heavy current densities affects on the low dimension region. This phenomenon can give rise to a heavy local temperature increase and, consequently, local diffusion or thermal breakdown, which may result in the solar cell destruction. That is why it is extremely important to avoid this degradation. Presented interpretation was supported by measurement of the reverse biased IV curves (see Fig. 4).

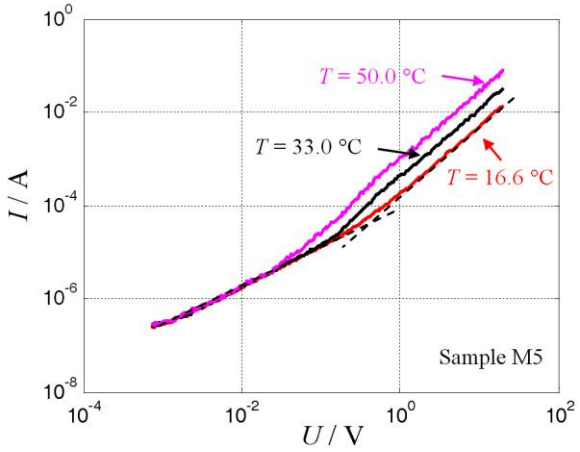

Fig.4. IV characteristics for diferent temperature, solar cell sample M5, dark enviroment.

The IV characteristic exhibits breakdown-like behaviour without abrupt increase of a current. The sample temperature was changed during the measurement and it turned out that the breakdown voltage (determined asymptotically) has negative temperature dependence. It again pointed out the temperature instability, [8]. Let's consider a local fluctuation of potential barrier (*pn* junction) conductivity. At a certain moment, when the heat transfer from the defect region is not sufficient, then a local heating induces thermal instabilities with gradual increase of the bias current. This process is followed by increase of the 1/*f* (flicker) noise in spectral characteristics, [9]. Nevertheless, defect-free part of the sample is stressed by the electric field and the dissipative power as well as the defect region. The sample background temperature also increases as depicted in Fig. 3b.

The power spectral densities of the sample M5 are depicted in Fig. 5a. Excess noise is very significant also in the low bias region where infrared radiation is under camera detection limit.

A noise spectrum exhibits the 1/f behaviour (except region close to the noise background) and it seems to be constant for the different voltage bias.

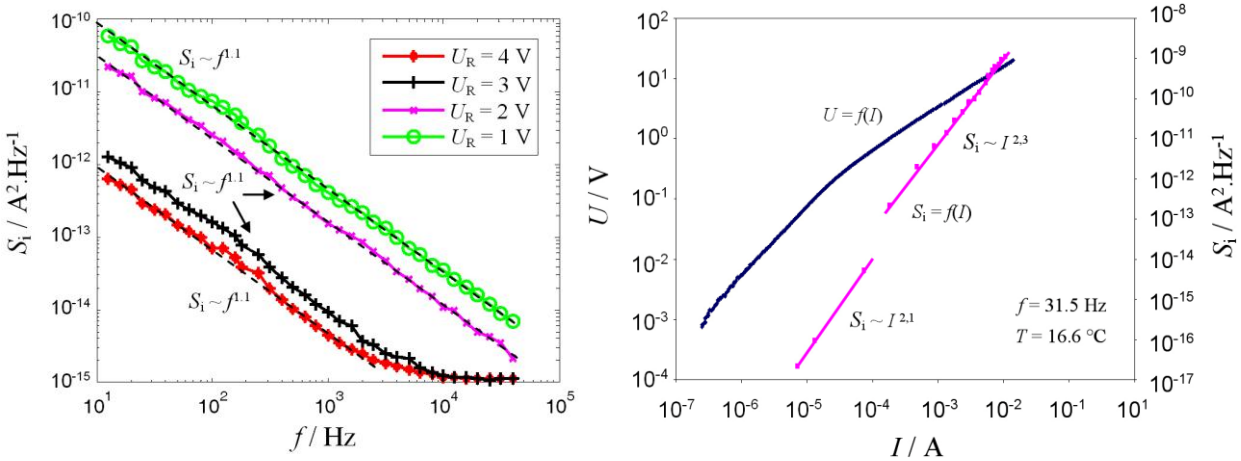

a) b)

Fig.5. a) Power spectral densities of current fluctuation for different bias voltage. Solar cell sample M5, dark environment and temperature T = 16.6 °C. b) Power spectral density at frequency f = 31.5 Hz as a function of bias current.

The flicker noise is modeled as a fluctuation in a macroscopic resistivity because of charge carriers mobility or number fluctuation. This process is mathematically described by an empirical Hooge formula as follows, [9].

$$\frac{S_R(f)}{R^2} = \frac{S_i(f)}{I^2} = \frac{S_u(f)}{U^2} = \frac{\alpha_H}{Nf^{\alpha}} \tag{1}$$

Here: R, I, U represent sample resistivity, bias current and bias voltage. α_H is the dimensionless Hooge constant, N number of fluctuating carriers and f frequency. This form of equation is valid only for homogeneous layers. The Hooge formula rigorous application and noise modeling is quite complicated issue for general inhomogeneous crystalline materials as well as solar cells, [10].

The local defect is possible to interpret as a region where the conductive channel is created after internal overheating. The conductivity of this channel is very early saturated and some limitation also introduces conductivity of semiconductor neutral parts. This effect is considered to be responsible for the linear-like IV characteristic after breakdown as we can observe in Fig. 4 and Fig. 6a. Fortunately, the excess current in the low voltage region seems to be also resistive although we are unable to predict the physical interpretation. Thanks to this fact, we are able to extrapolate excess current to the post-breakdown region and calculate current increase thought the conductive channel. This procedure is pointed out in Fig. 6a. The solid green line represents the total reverse current (I_{TOT}) through the sample, I_E (red line) represents the bulk excess current and finally I_{CH} (blue line) represents the current through defect spot. For the thermography analysis is possible to calculate defect dissipative current and introduce the modeling of internal temperature distribution. Let's pay attention back to the power spectral densities. The noise signal is very weak in the low bias voltage region where the thermal breakdown is not apparent. Nevertheless, it managed to get the PSD values for three bias levels (see Fig. 5a). Under investigation is now the PSD vs. bias current (see Fig. 5b). It turns out that this function is proportional to the bias current squared which correlates with the theoretical assumption according to Eq. (1). Following increase of the PSD is significantly supported at the moment of the breakdown (see Fig. 5b). However, the PSD is again

proportional to the bias current squared. Let us introduce assumption that the observed noise signal of the reference sample M5 is at first generated by the bulk semiconductor and finally by the defect region under electrical stress. We observe two independent noise processes in superposition. In the case of the defect region significant noise is supported by high flowing current and the small amount of active carriers (see quantity N in Eq. (1)). Note that the extracted slope of PSD characteristic in Fig. 5b is slightly higher after breakdown because of superposition of two processes.

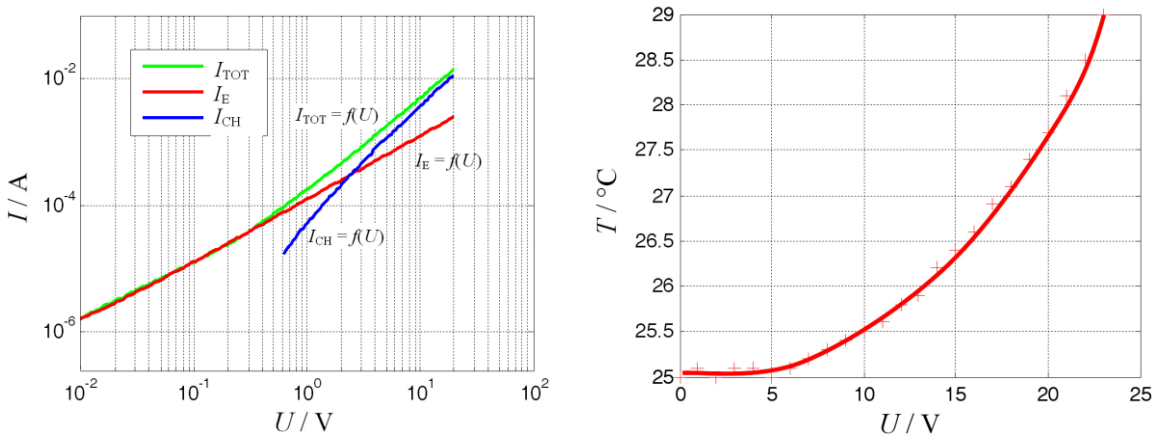

a) b)

Fig.6. a) IV characteristic of solar cell sample M5 and current extraction trought the defect region. Dark enviroment, temperature T = 16.6 °C. b) Tempererature characteristic as a function of applied bias voltage. Sample holder was kept at constant temperature T = 25.0 °C.

Next, it is interesting to study the defect spot temperature vs. voltage bias as depicted in Fig. 6b. It pointed out a parabolic character as may be expected because of the heat power at the constant resistance for various voltage (measurement has been done in the center of the defect region).

Microplasma local defects. Figure 7a depicts different fragment of the solar cell K20 with five spots emitting light. It should be emphasized here that the thermal activity of the sample is neglectable and the photon emission intensity is measured by means of the silicon CCD camera. The light spots again depend on the applied voltage and some of them are suddenly activated with the increasing DC electric field. Spectral analyses show that the PSD, which depends on the reverse voltage too, changes its character to generation-recombination spectrum (see Fig. 7b) but only for narrow interval of the bias voltage where is also optically activated spot 5 (see Fig. 7b). This behaviour is typical for the microplasma noise sources, [11], [12]. This assumption has been supported by observation in the time domain where the impulse Microplasma noise is suddenly created. Since other local inhomogeneties in a *pn* junction of the presented sample do not exhibit strong voltage dependence behaviour and it is not possible to distinguish particular noise contribution. The current noise power spectral density is again in the form of 1/*f* noise for the reverse voltage out from the microplasma instability region and pointed out rather the bulk thermal mechanisms. From a diagnostic point of view 1/*f* fluctuations may mask another noise sources.

Further information is possible to obtain from the optical spectrum measurement. Measurement has been done using accurate interference filters included into optical path. Optical filters properties (FWHM and insertion loss) weakly fluctuate with the center wavelength. On this account results are presented in relative units and as a reference point was choose the spot 1 at 1100 nm (see Fig. 8a). An interesting fact is that although the defect spots seems to have from noise point of view different nature, the optical spectrum of all light spots is very similar. Complications may arise because of optical absorption of bulk silicon.

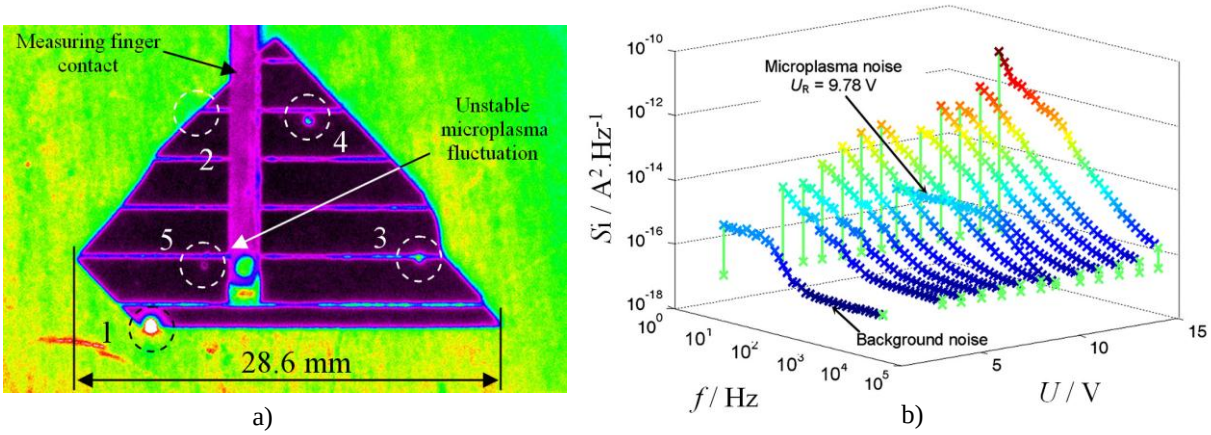

a) b)

Fig.7. a) Photography of measured solar cell with light defect spots, sample K20, reverse voltage U_R = 10 V, temperature T = 26.4 °C. b) PSD for various reverse voltages, sample K20.

The depth of the *pn* junction centre has been assessed as a 70 nm for our samples of solar cells (by means of differential capacitance profiling, [13]). It means that the source of light emission in the *pn* junction must be placed about 70 nm below the cell surface. Absorption coefficient, α, of the silicon is approximately $(1 \div 10^4)$ cm^{-1} at room temperature and operating wavelength range. That is why we suppose that we measure an original spectrum of light without distortion by silicon. The absorption coefficient of silicon to support this expectation is depicted in Fig.8b.

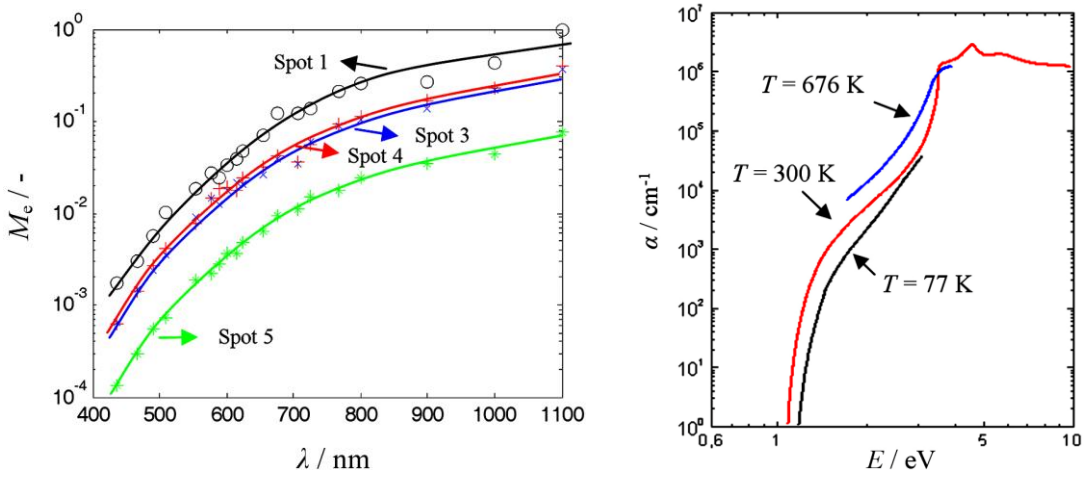

a) b)

Fig.8. a) Normalized light intensity M_e versus wavelength, FWHM is about 10 nm, reference value at 1100 nm and spot 1, sample K20, reverse voltage 13.4 V. b) The absorption coefficient of silicon vs. photon energy at different temperatures, adapted from [3].

What we measure is breakdown radiation due to impact ionization and avalanche multiplication. In this case, electrons are accelerated by electric field from *p* to *n* type semiconductor. Local regions become conductive in the reverse direction. The electron kinetic energy or the velocity has broad statistic distribution. On this account, inter-band recombination forms broad photon emission. The avalanche current typically decreases with the increasing temperature because of the limiting kinetic energy by collisions with the crystal lattice. Collisions are more likely because of increased thermal movement of the lattice. So, thermal dependence of radiation spectrum can be used for confirming of our assumption. Experimental verification of the radiation intensity temperature characteristics put forward comparable results as s optical spectrum for individual light spots (not presented here). Thank to this fact, we again expect that physical nature of the sample K20 defect regions is uniform

and comparable to microplasma. Individual noise contributions are probably masked below the bulk current fluctuation and it is still subject of our investigations.

Summary

The mechanism of reverse-biased junction conductivity appears to be due to crystalline lattice (structural) imperfections, dislocations, or metallic precipitates in the pn junction region. Local breakdowns will thus take place in the neighborhood of such defects at reverse voltages below those required for a breakdown in a defect-free region of the junction. Diagnostics of defect regions have been done by several methods which are measurement of IV characteristics, measurement of current noise signals for different reverse current or voltage bias and the sample temperature. Because of exposed solar cells pn junction it is possible put forward measurement of the radiation emitted from the defects during breakdowns and microplasma discharge formation.

We study both the deep infrared and the visible radiation of defects spots. It turns out that defects must be divided into specific groups with the consistent behaviour. Thermally active defects require quite comprehensive study of electrical noise and optical characteristics. We manage to get information about creating of conductive channels, noise contributions before and after the thermal breakdown and development of the defect spot temperature with the applied voltage bias. Similar investigations have been done also for different nature spots where microplasma discharges was indentified. Nevertheless, still it is not possible to put forward interpretation of all detected imperfections and our study will continue.

Acknowledgments

This paper is based on the research supported by the Grant Agency of the Czech Republic, the grant No. P102/10/2013, on the research supported by the Ministry of Industry and Trade of the Czech Republic, the project MPO TIP FR-TI1/305 and on the SIX research centre (project registration number: CZ.1.05/2.1.00/03.0072).

References

[1] European Commission, Joint Research Centre: Research, Solar Cell Production and Market Implementation of Photovoltaics, (2010), ISSN 978-92-79-15657-1.
[2] A. Luque, S. Hegedus: *Handbook of Photovoltaic Science and Engineering* (Chichester, England John Wiley & Sons 2002).
[3] P. Koktavy, J. Sikula: Fluctuation and Noise Letters, vol. 2, p. L65-L70, (2002).
[4] A.G. Chynoweth, G.L. Pearson: J. Appl. Phys., vol. 29, p. 1103 - 1110, (1958).
[5] O. Breitenstein, J.P. Rakotoniaina, M.H. Al Rifai, M. Werner: Progress in Photovoltaics, vol. 12, p. 529-538, (2004).
[6] P. Skaravada, P. Tomanek, L. Grmela, S. Smith: Solar Energy Materials and Solar Cells, vol. 94, p. 2358 - 2361, (2010).
[7] S.M. Sze: *Semiconductor Devices Physics and Technology* (John Wiley & Sons, Inc., 2002).
[8] M. Levinshtein, J. Kostamovaara, S. Vainhtein: *Breakdown Phenomena in Semiconductors and semiconductor devices*. (Singapore: World Scientific, 2005).
[9] P. Dutta, P.M. Horn: Rev. Mod. Phys., vol. 53, p. 497, (1981).
[10] R. Macku, P. Koktavy: Physica status solidi (a), vol. 207, p. 2387-2394, (2010).
[11] P. Koktavy, R. Macku, T. Trcka, B. Koktavy: presented at the 25th European Photovoltaic Solar Energy Conference, (2010).
[12] R.H. Haitz: J. Appl. Phys., vol. 35, p. 1370, (1964).
[13] R. Macku, P. Koktavy, P. Skarvada: WSEAS Transactions on Electronics, vol. 4, p. 192 - 197, (2008).